Jour. of the KGS, Vol. 22, No. 9. September 2006, pp. 15~22

Centrifuge Model Analysis on Mooring Line Deformation

닻줄변형에 관한 원심모형해석

Han, Heui-Soo[1] 한 희 수 Cho, Jae-Ho[2] 조 재 호
Chang, Dong-Hun[3] 장 동 훈 Jeong, Yeon-Koo[4] 정 연 구

요 지

선박을 정착시키기 위하여 해저지반에 관입된 드래그 / 영구앵커와 앵커에 연결된 닻줄의 지지력 및 변형을 해석하여, 기존의 앵커와 닻줄의 분석 및 개발을 위하여 만들어진 해석프로그램을 calibration 하기 위하여 원심모형시험기를 사용한 시험을 하였다. 시험에 사용된 닻줄은 ball chain 및 wire cable로써, 일정한 단면을 가지고 있으며, 해성점토 지반 안에 다양한 깊이로 정착시킨 후 원심모형시험을 실시하였다. 현장응력조건을 모사하기 위하여, 미리 응력을 가한 시험용 닻줄에 단계별 가속을 하였다. 이 논문은 닻줄의 해석을 위한 중요한 두 가지 변수인 닻줄과 지반의 부착력 및 접착면적환산계수를 결정하기 위한 과정을 설명하고자 하였으며, 이로 인한 닻줄의 변형 및 지지력 변화를 규명하였다.

Abstract

Single segmented mooring lines were tested in a geotechnical centrifuge for the purpose of calibrating the analytical solution developed for the analysis and design of various mooring lines associated with underwater drag/permanent anchors. The model mooring lines included steel ball chains and wire cables placed at various depths within the soft clayey seafloor soil. The mooring lines were loaded to preset tensions at the water surface under an elevated acceleration inside the centrifuge to simulate the field stress conditions experienced by the prototype mooring lines. This paper describes the calibration of two factors that are used as part of the input parameters in the analytical solution of mooring lines and considers the effect of chasing wires that were used in the experiment to determine the locations of the mooring lines.

Keywords : Centrifuge, Mooring line, Seafloor soil

1. Introduction

The U.S. Naval Facilities Engineering Service Center (NFESC) conducted a series of centrifuge model tests (Law, et al, 1994) on buried mooring lines in order to validate the analytical model developed by Bang (1996). During the centrifuge model tests a set of chasing wires were attached to the mooring chains and cables. Fig. 1 shows a schematic sketch of the layout of the mooring line and chasing wires. The chasing wires were used to locate the exact geometries of the mooring chains/cable during transition from the initial to the final position

1 Member, Associate Prof., Dept. of Civil Engrg., Kumoh National Uni. of Tec., hanhs@kumoh.ac.kr
2 Member, Ph.D. Candidate, Dept. of Civil Engrg., Kumoh National Uni. of Tec.
3 Member, Ph.D. Candidate, Dept. of Civil Engrg., Kumoh National Uni. of Tec.
4 Member, Associate Prof., Dept. of Civil Engrg., Kumoh National Uni. of Tec.

due to the applied load.

However, it was found later that the chasing wires had a rather significant effect on the mooring line geometry and tension, particularly on the mooring cable because of its thin cross section. This paper studies the effect of the chasing wires on the performance of the mooring line and the soil in calibrating the material and geometric parameters necessary for the validation of the analytical model.

2. Centrifuge Model Tests

The primary objective of the centrifuge model tests was to obtain the detailed load transfer mechanism of the mooring line embedded in a cohesive seafloor.

Therefore, the mooring lines were fixed at specific depths. They were tested under a centrifugal acceleration equal to 80 times the gravitational acceleration in order to simulate the nonlinear stress-dependent behavior of the soil. The tests included three ball chains and one cable embedded at various depths to model the mooring lines in Speswhite kaolin, a white potter's clay (Dunnavant and Kwan, 1993). The model ball chain had a ball diameter of 0.48 cm and was loaded to 208.52 N, and the model cable had a diameter of 0.48 cm and was loaded to 231.3 N horizontally at the seafloor surface. Note that the corresponding prototype geometric dimensions become model dimensions multiplied by the applied centrifugal acceleration level as a multiple of the gravitational acceleration. However, the corresponding prototype load is obtained by multiplying a square of the applied acceleration level.

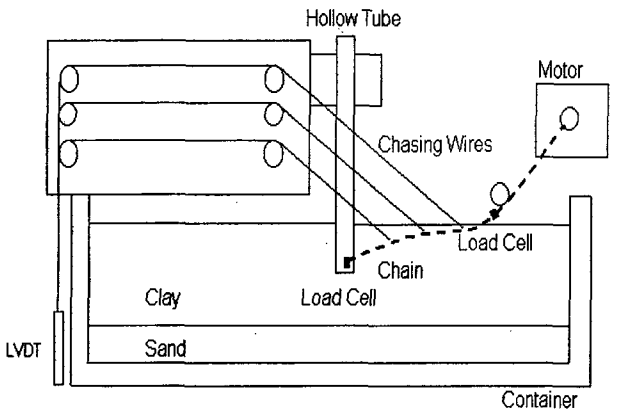

Fig. 1. Centrifuge Test Layout

A centrifuge at the University of Colorado, Boulder, Colorado, was used. It has a capacity of 440 g-tons with a capability of accelerating 2.2 ton payload to a maximum acceleration of 200 g's. It has a radius of 5.49 m from the centrifuge center to the top of the model bucket. The model bucket can be as large as 1.22 m x 1.22 m x 0.91 m.

The soil was first consolidated outside the centrifuge under a constant seepage force and then consolidated further within the centrifuge before the mooring lines were deployed. After the consolidation, the undrained shear strengths of the soil (S_u) were measured in-flight by a miniature vane and correlated with additional data derived from the void ratio versus shear strength relationship of the test clay (Law, et al, 1994). The results indicated that S_u remained constant at approximately 3112.2 Pa from the surface to a depth of 3.81 cm and then increased at a rate of 810.57 Pa/cm, indicating higher degrees of over-consolidation near the surface. This corresponds to S_u of 3112.2 Pa from zero to 3.05 m and 1021.06 Pa/m below 3.05 m in the prototype.

After the soil was consolidated, an individual tube with a mooring line attached to its end was inserted vertically into the soil until the mooring line end reached a desired depth. The exposed part of the mooring line above the soil surface was then connected to a step control motor located at a specified distance away from the tube and pulled under the elevated acceleration within the centrifuge until the line tension reached the specified load.

3. Description of Analytical Solution

The analysis of the static mooring line geometric configuration is based on the limiting equilibrium method in which the detailed solutions are obtained from the static equilibrium conditions. Fig. 2 shows a schematic diagram of a mooring line element embedded in the seafloor. T and ϕ are the axial tensile force and the inclination angle at the ends of the element. N, (f ds), and (w ds) are the normal force, the tangential force, and the buoyant weight of the mooring line element, respectively. From the static equilibrium conditions of forces along the "n" and "t"

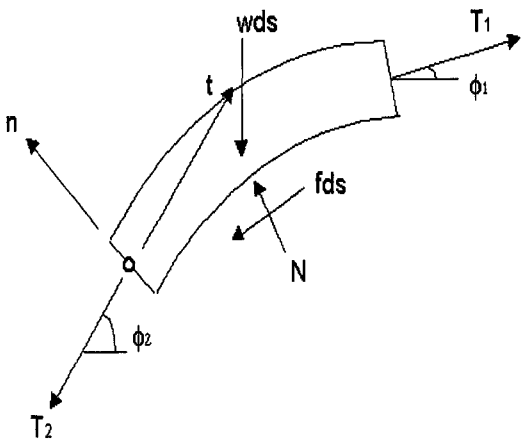

Fig. 2. Mooring Line and Free Body Diagram

coordinates and the moment about the point "o",

$$\Sigma F_t = 0$$
$$\Sigma F_n = 0$$
$$\Sigma M = 0 \qquad (1)$$

unknowns, N, T and ϕ, can be solved. Note that previously published solutions of the embedded mooring line analysis only considered partial equilibrium conditions (Brian Watt Associates, 1983; Degenkamp and Dutta, 1989; Vivatrat, et al, 1982). The current solution method utilizes complete equilibrium conditions and therefore permits an additional degree of freedom in each mooring line element.

In the analysis, it is assumed that the soil tangential forces (f ds) remain at their limiting state at all times, since the dominant mode of the mooring line movement during deployment is sliding. However, the normal soil forces (N) remain as unknowns because of the available additional degrees of freedom and, therefore, can be less than those defined by the limiting state, i.e., the soil bearing capacity.

Eq. (1) forms the basis of recursion formulas for the detailed analysis of the embedded mooring line element in the seafloor, i.e.,

$$T_2 = T_1 - (f + w\sin\phi_1)\,ds$$
$$N = \frac{2T_2 - f\,ds}{\tan\phi_1}$$
$$\phi_2 = \phi_1 + \frac{N - w\,ds\cos\phi_1}{T_2} \qquad (2)$$

where T_1 and T_2 = axial forces at the beginning and end of the element

f_1 and f_2 = mooring line inclination angle to the horizontal at the beginning and end of the element

f = tangential force per unit length of the element

w = buoyant weight of mooring line per unit length

N = normal force at the bottom of the element.

The solution process starts with a known mooring line inclination angle at the seafloor surface (ϕ_1). The catenary and embedded portions of the mooring line are then solved separately and added for the final solution.

With a known inclination angle at the seafloor surface and the horizontal force at the water surface, the mooring line axial tension at the seafloor surface (T_1) is calculated. Using Eq. (2), the axial tension and the inclination angle at the end of the element, T_2 and ϕ_2, are then calculated. The calculated orientation angle and the axial force at the end of the previous element become those at the beginning of the new element due to the compatibility requirements. However, when the chasing wire is attached, the orientation angle and the axial force at the beginning of the next element are altered as shown in Fig. 3. Because of the available equilibrium conditions, only two unknowns can be calculated.

The centrifuge test results include the values of the angles θ_c and θ_2, but not the forces T_c and T_2. Therefore, the force T_2 can be calculated from the equilibrium of forces at the point of the chasing wire attachment.

Fig. 3 shows a schematic diagram indicating the directions and magnitudes of forces acting at the attachment point. From the equilibrium of forces along the horizontal and vertical directions, the following equations are obtained.

$$T_2\cos\theta_2 + T_c\cos\theta_c = T_1\cos\theta_1$$
$$T_c\sin\theta_c + T_1\sin\theta_1 = T_2\sin\theta_2 \qquad (3)$$

where θ_1 = inclination of mooring cable before influenced by chasing wire

θ_c = inclination of chasing wire

θ_2 = inclination of mooring cable after influenced by chasing wire

T_1 = mooring cable force before influenced by chasing wire

T_c = force in chasing wire

T_2 = mooring cable force after influenced by chasing wire

These equations lead to

$$T_2 = T_1 \frac{\sin(\theta_1 - \theta_c)}{\cos\theta_c \sin\theta_2} \frac{\tan\theta_2}{\tan\theta_2 + \tan\theta_c} \quad (4)$$

T_2 in Eq. (4) is the adjusted axial force at the end of element considering the effect of the chasing wire.

In the recursion equations, the element tangential force per unit length, f, is estimated assuming that the soil undrained shear strength is fully mobilized, i.e.,

$$f = E_s\ D\ \alpha\ \beta\ S_u \quad (5)$$

where E_s = equivalent diameter conversion factor for sliding force to convert mooring line diameter to circumferential area

D = chain link or cable diameter

α = soil adhesion conversion factor

β = contact area conversion factor

S_u = soil undrained shear strength.

The soil adhesion conversion factor (α) is the ratio of the adhesion between the mooring line and the soil versus the soil cohesion. The contact area conversion factor (β) is the ratio of the true contact area between the mooring line and the soil versus the surface area of a cylinder defined by the mooring line.

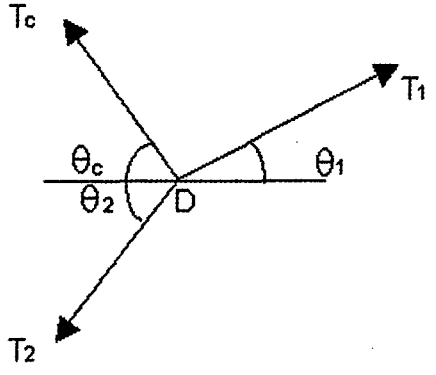

θ_1 = inclination of mooring cable before influenced by chasing wire

θ_c = inclination of chasing wire

θ_2 = inclination of mooring cable after influenced by chasing wire

T_1 = mooring cable force before influenced by chasing wire

T_c = force in chasing wire

T_2 = mooring cable force after influenced by chasing wire

Fig. 3. Definition of Angles and Forces

The value of the normal force, N, is limited to be no greater than the soil bearing capacity, i.e.,

$$N < N_{max} = q\ ds$$
$$q = E_b\ D\ S_u\ N_c \quad (6)$$

where q = bearing capacity of soil per unit length

E_b = equivalent diameter conversion factor for normal force to convert mooring line diameter to projected bearing area

N_c = soil bearing capacity factor.

The equivalent diameter conversion factor for normal force, E_b, can be obtained directly from the conversion of the mooring line geometry to the mooring line bearing area. For chains, the frontal area of the cylinder defined by a circle that encompasses the two perpendicular chain links can be used for the bearing area. For cables, the bearing area is the half cylinder defined by the cable.

The equivalent diameter conversion factor for sliding force, E_s, can be obtained directly from the conversion of mooring line geometry to the mooring line surface contact area. The circumference of a cylinder defined by chain links is (3.6 times π times D) / 12. For cables, the conversion can be made directly by dividing the circumference of the cable cylinder by the cable diameter.

The soil adhesion conversion factor, α, converts the soil cohesion into adhesion. For chains, the value of α can be taken as 1.0 due to the nature of the chain links formation. For cables, the value of α is a function of the soil undrained shear strength and can be estimated from the behavior of conventional piles.

The contact area conversion factor, β, is the ratio between the true contact area and the total available contact area between the mooring line and the soil while sliding. The value is taken as 1.0 for normally consolidated clay soils. If the mooring line starts to separate from the soil on its back side, the value of β could approach 0.5.

4. Mooring Cable Validation Study

The following input data were used for the mooring cable validation study. Note that the numbers inside the parenthesis indicate the prototype values, considering the acceleration level of 80 g's used in the centrifuge testing.

Mooring cable diameter = 0.48 cm (38.1 cm)
Diameter factor for cable bearing (E_b) = 1.0
Diameter factor for cable sliding (E_s) = 0.262
Mooring cable tension = 231.3 N (1480.29 kN)
Depth to fixed end = 15.24 cm (12.19 m)
Distance from fixed end to chasing wire attachment
point B = 4.69 cm (3.75 m)
point C = 10.78 cm (8.62 m)
point D = 18.37 cm (14.7 m)
point E = 25.87 cm (20.7 m)
Water depth = 0 (0)
Horizontal distance from fixed end to load application
34.29 cm (27.43 m)
Soil undrained shear strength
3112.2 Pa from 0~3.81 cm (0~3.05 m)
810.57 Pa/cm from 3.81 cm (1021.06 Pa/m)

Details of other parameters, such as the inclination angles of the chasing wires and the mooring lines as influenced by the chasing wires, are described by Bang (1998).

To validate the analytical solution, the effects of the following parameters have been studied: the bearing capacity factor for cables (N_{cw}) and the product of the soil adhesion conversion factor for cables (α_w) and the cable contact area conversion factor (β_w). This was because the tangential force developed at the bottom side of the mooring line was influenced by the product of α_w and β_w and no attempt was made to separate the effects of these two parameters during the model test.

Fig. 4 shows the effect of N_{cw} on the mooring cable geometry. Note that the value of $\alpha_w\beta_w$ is 1.0 for all values of N_{cw}. It indicates that the effect of Ncw is relatively insignificant for the magnitudes considered (N_{cw} = 7~13). Values of N_{cw} between 7 and 9 provide very good comparisons with the experimental measurement. As the value of N_{cw} increases, the mooring cable profile tends to shift upward. All test results including Test 1-4 are multiplied by 80 for prototype dimensions,

Fig. 5 shows the effect of $\alpha_w\beta_w$ on the mooring cable geometry with N_{cw} of 9. The results indicate that the influence of $\alpha_w\beta_w$ is virtually nonexistent when the value of $\alpha_w\beta_w$ varies from 0.5 to 3.2.

Fig. 6 shows the changes in mooring cable forces at the ground surface ($T_{surface}$) and at the fixed end (T_{anchor}) as a function of $\alpha_w\beta_w$. Note that the measured mooring cable force at the fixed end is 1,170,001.92 N.

Results indicate that the mooring cable geometry as influenced by the chasing wires can be estimated very accurately using the values of N_{cw} = 7~9 and $\alpha_w\beta_w$ = 0.5~3.2. However, the measured mooring cable force at the fixed end is significantly influenced by the values of

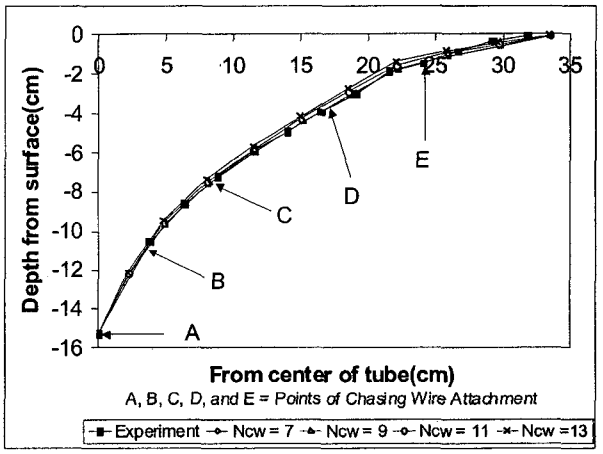

Fig. 4. Mooring Line Geometry with Various Values of N_{cw}

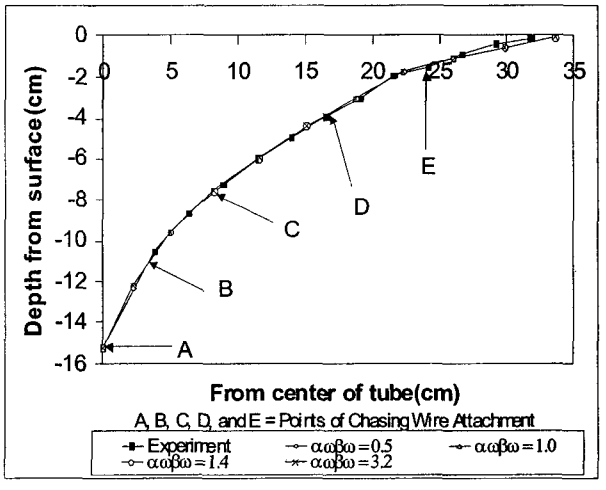

Fig. 5. Mooring Line Geometry with Various Values of $\alpha_w\beta_w$

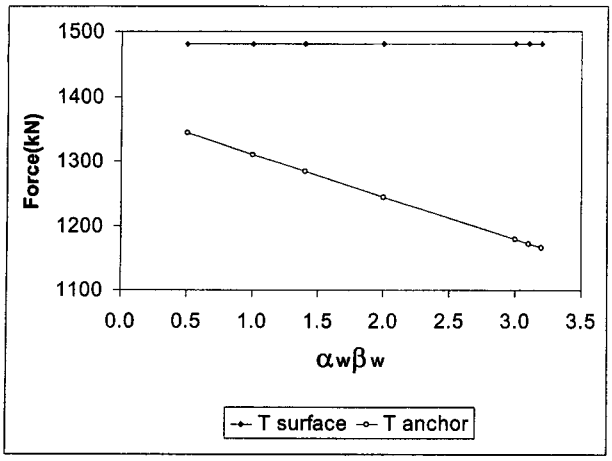

Fig. 6. Mooring Cable Force Variation with $\alpha_w\beta_w$

N_{cw} and $\alpha_w\beta_w$. The measured mooring cable force at the fixed end could be obtained if the values of $\alpha_w\beta_w$ of 3.2 and N_{cw} of 9 are used.

5. Mooring Chain Validation Study

The following input data were used for the mooring chain validation study. The numbers inside the parenthesis indicate the prototype values, considering the acceleration level of 80g's used in the centrifuge testing. Ball chain was used to model the mooring chain.

Ball chain diameter = 0.48 cm
Equivalent mooring chain link diameter = 13.61 cm
Diameter factor for chain bearing (E_b) = 0.233
Diameter factor for chain sliding (E_s) = 0.733
Mooring chain tension = 208.61 N (1,334.4 kN)
Depth to fixed end
5.08 cm (4.06 m) for test 1-1
10.06 cm (8.13 m) for test 1-2
15.24 cm (12.19 m) for test 1-3
Water depth = 0 (0)
Horizontal distance from fixed end to load application
24.13 cm (19.3 m) for test 1-1
31.75 cm (25.4 m) for test 1-2
36.83 cm (29.47 m) for test 1-3
Soil undrained shear strength
3112.2 Pa from 0~3.81 cm (0~3.05 m)
810.57 Pa/cm from 3.81 cm (1021.06 Pa/m)

As indicated in the mooring cable analysis, the effects of the soil adhesion conversion factor for chains (α_c) and the chain contact area conversion factor (β_c) were combined.

To narrow down the variations in input parameters, a preliminary analytical parametric study was conducted using the developed solution method. From the preliminary parametric study, it was concluded that the optimum value of the bearing capacity factor for chains (N_{cc}) that matches the mooring line trajectories lies between 13 and 17, and the optimum value of $\alpha_c\beta_c$ lies between 1 and 2. The trajectories tend to shift upward as the value of N_{cc} increases, with virtually no influence from the change in value of $\alpha_c\beta_c$. However, the value of $\alpha_c\beta_c$ has a significant effect on the mooring chain force at the fixed end. In general, as the value of $\alpha_c\beta_c$ increases, the force at the fixed end decreases.

To determine the optimum value of $\alpha_c\beta_c$, second vector norms of error in $\alpha_c\beta_c$ were calculated for various N_{cc} values and they were used to calculate the optimum values of $\alpha_c\beta_c$ at given N_{cc}, as shown in Table 1. A linear regression analysis with a second order polynomial indicated that the value of $\alpha_c\beta_c$ of 1.45 produced the optimum value.

To study the effect of the value of N_{cc} on the mooring chain geometry, the trajectory of each mooring line was compared with predictions with various values of N_{cc} varying from 13 to 17 but with the fixed, optimum value of $\alpha_c\beta_c$ of 1.45. One such example is shown in Fig. 7, which compares the measured mooring chain trajectory of Test 1 -3 of those calculated with various values of N_{cc}. The effect of N_{cc} on the mooring chain trajectory is clearly observed from the figure. The mooring chain

Table 1. Optimum Values of $\alpha_c\beta_c$

N_{cc}	$\alpha_c\beta_c$
13	1.448
14	1.445
15	1.451
16	1.444
17	1.441
$\alpha_c\beta_c$, ave. =	1.45

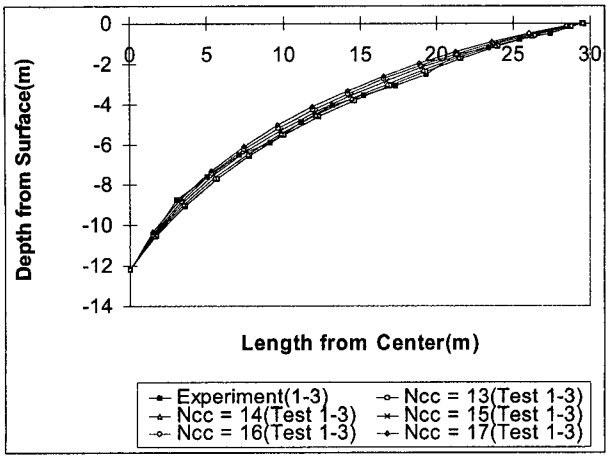

Fig. 7. Mooring Line Geometry of Test 1-3 with N_{cc} Variation ($\alpha_c\beta_c$ = 1.45)

Table 2. Comparisons of Measured and Calculated Forces at Anchor ($\alpha_c\beta_c$ = 1.45)

Test No.	T_{test} (kN)	N_{cc}	T_{anchor} (kN)	Error
		13	1219.1	−0.101
		14	1218.21	−0.100
Test 1-1	1107.37	15	1217.39	−0.099
		16	1215.43	−0.098
		17	1214.82	−0.097
		13	1126.94	−0.271
		14	1123.44	−0.267
Test 1-2	886.47	15	1123.18	−0.267
		16	1121.6	−0.265
		17	1120.22	−0.264
		13	1005.86	0.036
		14	1003.69	0.039
Test 1-3	1043.89	15	1003.3	0.039
		16	1003.03	0.039
		17	1002.9	0.039

trajectory shifts upward as the value of N_{cc} increases. Overall, the value of N_{cc} of 14 produces the best results when all test results are considered.

Table 2 shows the comparisons of measured and calculated mooring chain forces at the fixed end (T_{anchor}). $\alpha_c\beta_c$ value remained as 1.45, since it was determined to be the optimum value. As can be seen from Table 2, it is apparent that the force at the fixed end is not influenced much by the value of N_{cc}. Errors were calculated from

$$\text{Error} = \frac{T_{test} - T_{anchor}}{T_{test}}$$

Please note that the experimental results of Test 1-2 should not be taken as indicative. The results are questionable when they are compared to those of Tests 1-1 and 1-3, comparing the anchor depth.

Results of Tests 1-1 and 1-3 indicate that the mooring chain trajectory is primarily influenced by the value of N_{cc}, whereas the force at the fixed end is primarily influenced by the value of $\alpha_c\beta_c$. The mooring chain geometry and the force at the fixed end as influenced by the chasing wires can be estimated with reasonable accuracy using the values of N_{cc} = 14 and $\alpha_c\beta_c$ = 1.45.

6. Conclusion

From the results of the validation study, the optimum values of N_c and $\alpha\beta$ have been determined as follows.

For mooring cable, N_{cw} = 9

$$\alpha_w\beta_w = 3.2$$

For mooring chains, N_{cc} = 14

$$\alpha_c\beta_c = 1.45$$

The optimum value of N_c for the mooring cable is very close to that predicted by conventional foundation bearing capacity theories, whereas the optimum value of N_c for mooring chains is higher. The reason is not perfectly clear and needs to be studied in detail in the future.

It is noted that N_{cc} = 13 and $\alpha_c\beta_c$ = 1.4 were obtained in the previous study (Bang, et. al, 1996) which did not consider the effect of chasing wires on mooring chains. Although the differences in values of N_{cc} and $\alpha_c\beta_c$ are noted with and without considering the effect of chasing wires, the difference is not significant for mooring chains. However, the effect of chasing wires is significant on mooring cables. In future centrifuge tests, better instrumentation technique of locating the mooring line geometry should be used to eliminate completely the effect of chasing wires.

It is noted that these values have been determined from comparisons with the centrifuge test results on mooring

lines with chasing wires. Therefore, the use of these values for mooring lines with no chasing wires may not be applicable. It is also noted that the soil used in model tests was consolidated within the centrifuge and therefore no effort was made to simulate other time dependent behaviors of soil such as aging. The results presented in this paper have been drawn based on a limited number of centrifuge model tests. Additional tests may be needed to validate the conclusions provided.

Acknowledgement

The authors are grateful to the technical and financial supports provided by Kumoh National University of Technology.

References

1. Bang, S (1996), "Anchor Mooring Line Computer Program User Manual", Contract Report CR - 6020 - OCN, Naval Facilities Engineering Service Center.
2. Bang, S (1998), "Use of Suction Piles for Mooring of Mobile Offshore Bases", Quarterly Progress Report prepared for Naval Facilities Engineering Service Center.
3. Bang, S, and Taylor, RJ, Jie, Y, and Kim, HT (1996), "Analysis of Anchor Mooring Line in Cohesive Seafloor", Transportation Research Record, No.1526.
4. Brian Watt Associates, Inc (1983), "A Method for Predicting Drag Anchor Holding Capacity", Report No. CR 83.036.
5. Degenkamp, G, and Dutta, A (1989), "Soil Resistance to Embedded Anchor Chain in Soft Clay", *Journal of Geotechnical Engineering*, Vol.115, No.19.
6. Dunnavant, TW, and Kwan, CTT (1993), "Centrifuge Modeling and Parametric Analysis of Drag Anchor Behavior", *Offshore Technology Conference Paper* No.7202.
7. Law, HK, et al. (1994), "Centrifuge Testing for Dynamic Anchor Line Modeling", A Report submitted to Naval Facilities Engineering Service Center, Univ. of Colorado, Boulder.
8. Vivatrat, V, Valent, PJ, and Ponterio, AA (1982), "The Influence of Chain Friction on Anchor Pile design", *Proc., 14th Annual Offshore Technology Conference*, Paper No.4178.

(received on Jan. 31, 2006, accepted on Sep. 20, 2006)